

**SUPRAGLACIAL STREAM DYNAMICS
ON THE JUNEAU ICEFIELD, ALASKA**

by

R.A. Marston

**Juneau Icefield Research Program
Foundation for Glacier and Environmental Research
and
Department of Geology, University of Texas, El Paso**

**Annals of the Association of American Geographers
Vol. 73, No. 4, pp. 597-608
1983**

Supraglacial Stream Dynamics on the Juneau Icefield

Richard A. Marston

Department of Geological Sciences, University of Texas at El Paso, El Paso, TX 79968

Abstract. Measurements of discharge, reach morphology, and cross-section morphology in supraglacial streams on the Juneau Icefield reveal controlling variables that have analogous counterparts in alluvial streams. Downward sky radiation imparts a strong diurnal pattern to supraglacial runoff generated by saturated slush flows, precipitation and melting, channel erosion, and spillover from water-filled moulins, crevasses, and supraglacial lakes. Supraglacial streams are generated when runoff is concentrated on glacier slopes and rates of incision exceed rates of glacier surface ablation. Streams leave the surface via moulins and crevasses where the water becomes part of the englacial and subglacial drainage systems. Meander systems develop and migrate downstream, driven by thermal erosion with heat supplied by climatic and hydrologic sources. Sinuosity attains a maximum value, in the absence of other roughness factors, when high stream power is imposed from an adjacent upstream reach. Form-process relationships for supraglacial meanders are similar to those for alluvial streams in spite of the contrast in time and scale of development. At-a-station hydraulic geometry for supraglacial streams serves to identify channel adjustments to changing discharge not unlike those for narrow-deep, straight alluvial streams. Daily formation of longitudinal grooves in channel walls leaves a record of daily flow and yields critical information regarding channel enlargement ratios. Fluvial adjustment toward equilibrium conditions involves all elements of channel roughness and cannot be analyzed using any single indicator such as channel pattern, cross-sectional shape, or materials involved.

Key Words: supraglacial streams, glacial meltwater, meanders, channel roughness, hydraulic geometry, Juneau icefield.

SURFACE meltwater below the *névé* line on temperate, stagnant glaciers will carve supraglacial (superglacial) streams if the rate of channel downcutting exceeds the rate of glacier surface ablation. Supraglacial streams merit investigation because they adjust in a similar manner to, but much faster than, alluvial streams. The primary objective of the present study is to identify controlling variables in supraglacial streams that have analogous counterparts in alluvial streams. A secondary objective is to examine form and process that are intrinsic to supraglacial streams, including integration of supraglacial water with other portions of the multi-level, glacio-hydrologic drainage system.

Research was conducted over two summer field seasons on the Juneau Icefield, situated in the Alaska-Canada Boundary Coast Range,

east of lower Lynn Canal and north of the Taku River and Juneau, Alaska (Fig. 1). Covering an area of approximately 4,000 km², the Juneau Icefield is a remnant of the Cordilleran ice sheet, and its direction of ice movement is controlled by the underlying topography. More than 30 outlet glaciers drain the icefield, but only Taku and Hole-in-the-Wall are advancing. Two research areas on the icefield were selected for field sites. The Lemon Creek-Ptarmigan Glacier Research Area includes sites at elevations of 850 m and 1,200 m on the western edge of the icefield.¹ The Vaughan Lewis-Gilkey Glacier Research Area lies in a more continental climatic setting at an elevation of 1,100 m. The mean *névé* line reaches 1,090 m on Lemon Creek Glacier and 1,280 m on Vaughan Lewis Glacier (Miller 1975). The Juneau Icefield is de-

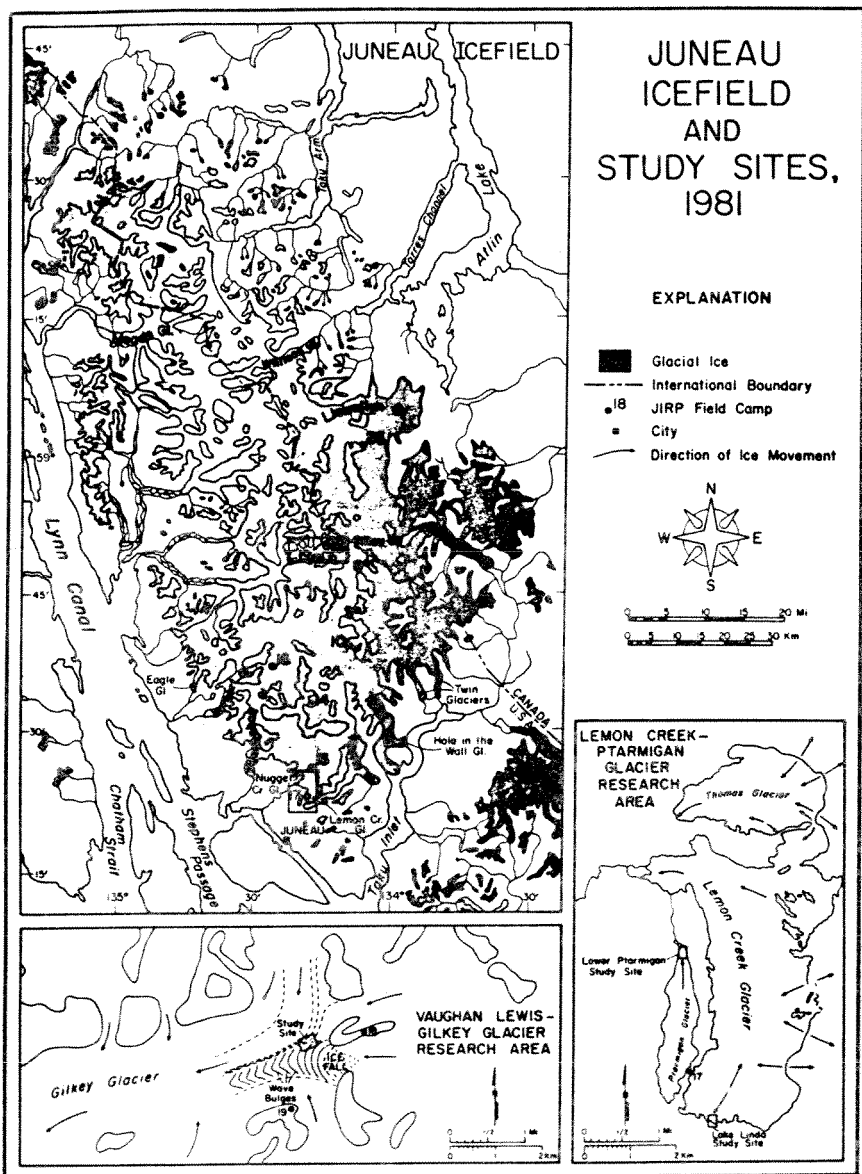


Figure 1. Location of research areas, Juneau Icefield, southeast Alaska-northwest British Columbia.

scribed in detail by Marcus (1964) and Miller (1963, 1964, 1975).

Supraglacial streams are best developed in stagnant ice areas. Ferguson (1973) and Park (1981) focus on the sinuosity and hydraulic geometry, respectively, of supraglacial streams on a Swiss valley glacier. Knighton (1972) examines the meander geometry of supraglacial streams in Norway. Parker (1975) and Pinchak (1972a, 1972b) derive models to explain thermal degradation in supraglacial streams. Dozier (1976) uses measurements of bed shear stress to test whether supraglacial streams adjust according to the principle of minimum variance. Leopold and Wolman (1960) and Zeller (1967) include supraglacial streams in their systematic studies of meandering in alluvial rivers. Other research begins to define the relationship of supraglacial water to englacial and subglacial drainage networks (Clayton 1964; Price 1973). Particular attention is given to the evolution of moulins and the hazard of glacier outburst floods (Streiff-Becker 1951; Glen 1954; Dewart 1966; Howarth 1968). The present study reviews past findings and theories concerning supraglacial runoff and stream morphology in the light of new data. Moreover, a systematic analysis of supraglacial channel roughness is seen as a key, and previously unstudied, element of supraglacial stream dynamics.

Supraglacial Runoff

Supraglacial water is derived from four sources. First, daytime melting in the névé (area covered by perennial snow or firn) produces water at a rate exceeding the infiltration capacity of the dense firn. Nighttime radiation cooling of the snowpack may create a hard surface crust, resulting in a saturated slush flow between the crust and firn. Supraglacial water produced in this manner occurs on gentle glacier slopes at the stage of the ablation season when old snow is 10–20 cm thick over firn, and is prolonged when cloudy days follow clear sky nights. Ferguson (1973) and Dozier (1976) support claims that saturated slush flows reopen former supraglacial channels. Use of fluorescent dye in saturated slush flows in the Lake Linda study area demonstrates that microrelief concen-

trates the slush flow, although rates of flow do not exceed 5 percent of overcrust flow rates on the same glacier slope.

The second source of supraglacial water is precipitation and melting below the névé line. Surface runoff on a glacier slope leads to the formation of rills that combine into channels carved in firn and later superimposed on glacier ice.

Melting of the channel bed and banks by streamflow in existing channels provides the third source of supraglacial water. Channel initiation and expansion requires thermal erosion; a temperature of 0.005 to 0.01°C can account for observed rates of incision between 3.8 and 5.8 cm/day (Pinchak 1972a, 1972b). Parker (1975) and Ferguson (1973) claim that heat derived from viscous flow dissipation accounts for the necessary heat supply, but energy budget models by Pinchak (1972a, 1972b) point to the need for steep channel gradients before frictional heat can provide the necessary heat of fusion. In an example calculation, Pinchak (1972a) reports a channel gradient of 20 percent necessary to produce the heat required for melting in a supraglacial stream with a width of 0.6 m and discharge of 56 l/s. Gradients of this magnitude are found only where streams drop into a moulin or crevasse.

The fourth source of supraglacial water involves spillover from water-filled moulins, crevasses, and supraglacial lakes. Supraglacial water leaves the glacier surface via moulins and crevasses that impose a local base level on the stream.

Hydrograph Characteristics

The production of supraglacial runoff can be related to downward sky radiation for a six-day interval in 1981 (Fig. 2). Downward sky radiation is measured with a pyranometer sensitive to 90 percent of radiation from 0.36 to 2.0 μm , 50 percent of radiation at 3.3 μm , and 20 percent at 40 μm . Stage-discharge rating curves were constructed for three streams in the Vaughan Lewis-Gilkey Research Area in order to derive hydrographs. This task was accomplished using pygmy current meters, fluorescent dye, and staff gages. The three streams transect medial moraines at the confluence of the Vaughan

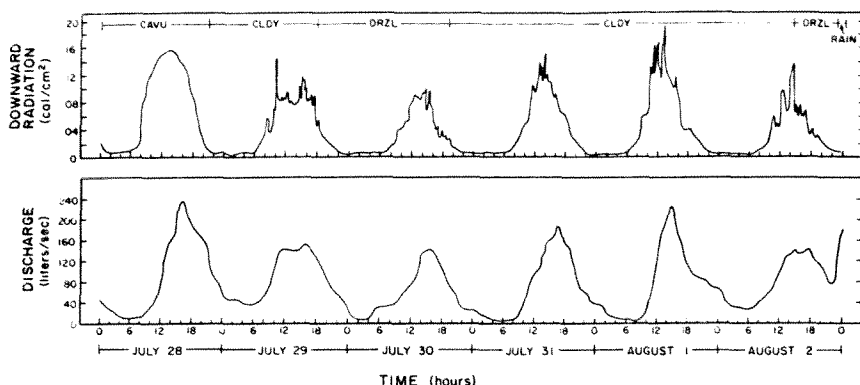


Figure 2. Sky conditions, downward sky radiation and discharge for one of the supraglacial streams in the Vaughan Lewis-Gilkey Glacier Research Area. CAVU denotes clear and visibility unlimited, CLDY cloudy, and DRZL drizzle.

Lewis and Gilkey Glaciers (Fig. 1). Drainage area for the three streams ranges from 40 to 60 ha. Crevasse patterns related to the confluence and wave bulges at the base of the Vaughan Lewis Icefall exert strong controls on supraglacial channel orientation. A correlation matrix reveals the interrelationships

between climatic, hydrologic, and morphologic variables (Table 1).

Peak daily discharge ranged between 140 and 230 l/s and is most closely correlated with peak downward radiation ($r = 0.928$) in the absence of measurable precipitation. The lag time between peak downward radiation and

Table 1. Correlation Matrix with Downward Sky Radiation and Supraglacial Stream Dynamics, Vaughan Lewis-Gilkey Research Area

	CDC	GSA	VGD	HGD	PDR	TDR	PDS	TDS
Channel Downcutting (CDC)	1.000	0.572 0.118*	0.915 0.005	0.480 0.168	0.727 0.051	0.729 0.050	0.856 0.015	0.366 0.238
Glacial Surface Ablation (GSA)		1.000	0.686 0.066	0.787 0.032	0.698 0.062	0.525 0.143	0.520 0.145	0.748 0.044
Vertical Groove Depth (VGD)			1.000	0.730 0.050	0.832 0.020	0.754 0.042	0.871 0.012	0.632 0.089
Horizontal Groove Depth (HGD)				1.000	0.746 0.044	0.750 0.043	0.642 0.085	0.946 0.002
Peak Downward Radiation (PDR)					1.000	0.826 0.021	0.928 0.004	0.822 0.022
Total Downward Radiation (TDR)						1.000	0.916 0.005	0.715 0.055
Peak Discharge Daily (PDS)							1.000	0.649 0.081
Total Discharge (TDS)								1.000

* Probability that $r = 0.0$ in the population.

peak daily discharge remained at approximately two hours regardless of sky conditions. The lag can be attributed to the time needed to accumulate latent heat of fusion required for melting glacier ice. The rising limb of hydrographs is generally steeper than the receding limb. In the morning, meltwater production per unit area and source area are both increasing. In the afternoon, meltwater production per unit area decreases while the source area continues to expand. Channel downcutting and groove dimensions as a function of discharge are discussed later.

Total daily discharge ranged from 515×10^3 to 763×10^3 l/day and is more closely correlated with peak downward radiation ($r = 0.916$) than with total downward radiation ($r = 0.715$). Crude daily sketches of the active trellis drainage network point to a link between variable source area and total daily discharge, with the source area responding to peak downward radiation.

Lake Linda

The link between supraglacial, englacial, and subglacial water can be examined in the vicinity of Lake Linda in the Lemon Creek-Ptarmigan Glacier Research Area (Fig. 1). Lake Linda is a supraglacial lake at the head of Lemon Creek Glacier that drains suddenly each summer through a composite englacial cave 450 m long (Fig. 3). Glen (1954), Howarth (1968), and Rothlisberger (1972) attribute rapid and catastrophic release of supraglacial lake water to increasing water depth beyond a threshold when hydrostatic pressure exceeds compressive strength of ice on the lake bottom. In the specific case of Lake Linda, the critical factor may be the tensile strength of the bond between glacier ice and headwall moraine debris on the lake bottom. The ice fractures and becomes buoyant, opening the cave entrance. Later, the entrance is blocked by icebergs as lake water drains. The notion of a water depth threshold is supported by the fact that the cave opening is at the deepest part of the lake. Water floods the cave to create an extensive englacial reservoir, eventually leaving through subglacial drains in the cave floor. Streamflow surges recorded in Lemon Creek below the glacier terminus may be related to the sudden release of Lake

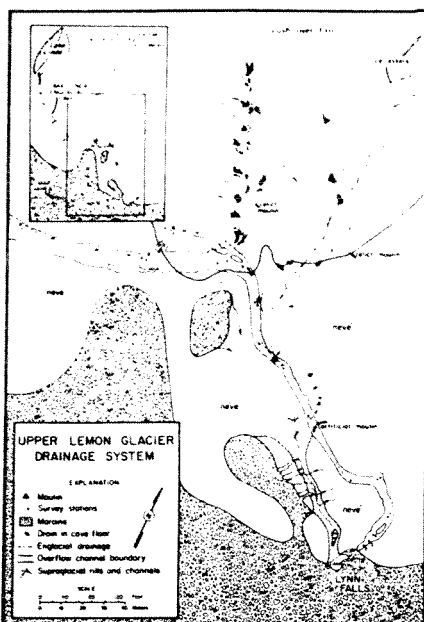


Figure 3. Linkage between supraglacial, englacial, and subglacial drainage systems in Lake Linda study site. Lake Linda englacial cave originally surveyed by Asher et al. (1974).

Linda water (Miller 1975). Spectacular ice speleothems, sublimation features, and black glacier ice are revealed by a cave traverse following drainage of Lake Linda.

Plan-view and longitudinal maps of Lake Linda are presented by Asher et al. (1974) from their survey of the cave under difficult conditions. During the course of the present study, cave survey stations were projected onto a hydrologic map of the glacier surface (Fig. 3). Fluorescent dye placed in rills and channels that empty into moulines and crevasses reveals links between the supraglacial, englacial, and subglacial drainage. An artificial moulin drilled near survey station 8 for radio communications in the cave fills with snow during the winter, blocking the cave in a manner described by Dewart (1966). When Lake Linda drains the following summer, water backs up under hydrostatic pressure in the cave, reopening a large moulin between stations 9 and 10 (Fig. 3). Water from the cave spills onto the glacier surface at this point,

creating a supraglacial overflow channel leading toward Lynn Falls.

Supraglacial Stream Morphology

A small but discrete supraglacial stream on lower Ptarmigan Glacier is re-established each year on mudflow debris. The mudflow originated from a mass-wasting event in the early 1970s on the west-facing valley wall and is re-exposed each summer by ablation. With a thickness (approximately 1 cm) insufficient to insulate the ice, the mudflow debris absorbs shortwave radiation and then conducts sensible heat to the ice, accelerating melting along the narrow downslope path of the mudflow. The lower Ptarmigan stream is divided into 16 reaches based on shifts in sinuosity, channel shape, glacier slope, discharge, and presence or absence of reworked mudflow debris in the active channel. Stationary and symmetric ridges of ice are carved into the channel bed in several reaches. These carved-ice bedforms are transverse to the flow direction and cause undulations in the water surface profile.

Channel Patterns

Straight channel segments are restricted to supraglacial streams controlled by crevasse orientation or located on steep glacier slopes. Braided segments are usually found as rills on glacier slopes where thermal erosion by the water in rills barely exceeds glacier surface ablation, so that channel capacity cannot expand at the rate of morning increases in meltwater production. Meanders are well developed in the study sites where channel downcutting proceeds at rates more than twice the rate of glacier surface ablation. Meander wavelengths in the lower Ptarmigan stream are very short (135-500 cm), but small amplitudes restrict sinuosity to values between 1.05 and 1.25. Nevertheless, definite breaks in sinuosity are evident with shifts in one or more of the other variables used to delineate reaches; these are indicative of systematic morphological and process controls. Contrary to claims by Parker (1975), supraglacial meanders do migrate downstream while downcutting, leaving a visually impres-

sive record of the meander belt on channel sidewalls. Abandoned meander loops are also formed when cutoffs are created while the channel is rapidly downcutting.

Stream power per unit bed area P_j/A and stream power per unit channel length P_j/L are calculated using the following formulae: $P_j/A = \gamma RSV$ and $P_j/L = \gamma QS$, where γ is the specific weight of water, R the hydraulic radius, S the slope of the water surface, V the velocity, and Q the discharge. Stream power per unit bed area and glacier slope respectively explain only 49.8 percent ($SE = 0.037$) and 68.9 percent ($SE = 0.029$) of the variance in sinuosity (Fig. 4). Stream power per unit channel length offers little additional explanatory power ($r^2 = 0.597$, $SE = 0.031$) and values are generally an order of magnitude higher for a given sinuosity than reported by Schumm (1977) using flume data. Close inspection of the ice at the lower end of highly sinuous supraglacial reaches reveals ice structures that may retard the downglacier migration of the meander system. Recrystallization of water in ice fractures can create a density barrier, causing meanders to "pile up" and generating a higher sinuosity than expected for observed values of stream power or glacier slope. This situation is analogous to the effect of resistant clays in the lower Mississippi River Valley retarding downstream migration of that meandering system (Kolb 1963).

The relationships between meander wavelength and discharge and between wavelength and channel width reflect the role of secondary circulation in meander morphology (Fig. 5). Fluorescent dye may be used to detect helical flow in supraglacial streams. Of particular interest is the separation of data into two groups, depending on whether clastics are present in the channel from reworked mudflow deposits. The slope of the curve for the debris-free reach data agrees closely with values reported by Leopold and Wolman (1960) and Zeller (1967) for supraglacial streams and with values for alluvial streams summarized by Shahjahan (1970). It is believed that debris in the active channel provides the roughness necessary for shorter meander wavelengths. In the absence of debris, wavelength and stream power increase unless kinetic stream energy is dissipated by other elements of channel roughness.

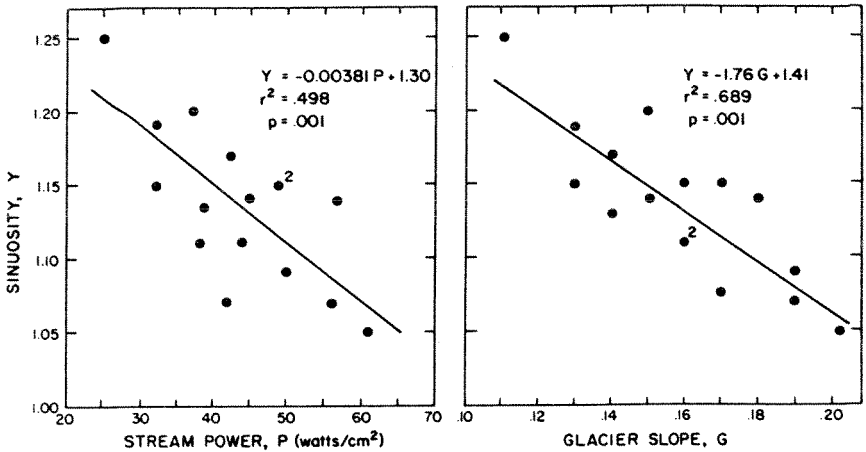


Figure 4. Inverse sinuosity relationships with stream power per unit bed area and glacier slope for the 16 lower Ptarmigan supraglacial stream reaches.

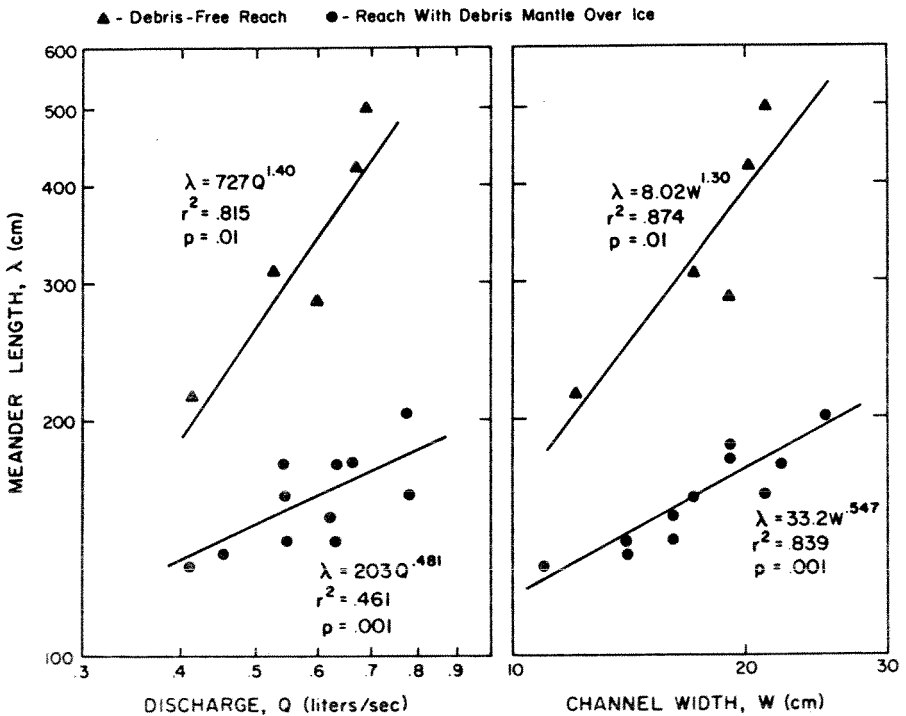


Figure 5. Meander wavelength relationships with discharge and channel width for the 16 lower Ptarmigan supraglacial stream reaches.

Ferguson (1973) claims that maximum sinuosity develops in supraglacial streams with the highest initial rates of power expenditure. Indeed, data from the lower Ptarmigan stream indicate that sinuosity increases in the downstream direction as the adjacent upstream reach supplies a higher stream power per unit bed area. Random irregularities related to differential ice crystal density impart asymmetry to the helical flow, causing water surface super-elevation against one bank. This increment of water depth and associated shear stress may provide frictional heat sufficient to accelerate thermal erosion on the outside of bends and freezing on the inside of bends (Parker 1975, 1976). Differential melting and freezing caused by differential frictional heat associated with secondary currents need not account for all observed downcutting, but it does explain the initiation and migration of meanders. Pinchak (1972a, 1972b) and Dozier (1976) demonstrate that sensible heat flux to the stream from the air along with the transmission and absorption of shortwave radiation can account for 75 to 100 percent of all downcutting. In the present study, incision rates range from 4 to 8 cm/day, whereas glacier surface ablation rates range from 1 to 4 cm/day. Therefore, climatic processes account for 25 to 50 percent of incision rates.

Channel Roughness

Mutually interdependent elements of channel roughness can be quantified for supraglacial streams. The potential stream energy per unit mass of water is proportional to the relief in each reach. Vertical-fall obstructions in a stream reduce the potential stream energy available for conversion to kinetic stream energy, which is needed to transport imposed water and sediment supplies (Marston 1982). No vertical-fall obstructions are present in the lower Ptarmigan stream. Kinetic stream energy is dissipated by particle roughness (skin resistance) and form roughness. The latter involves geometry of the channel bed, channel pattern, and channel cross-section shape. The undissipated kinetic stream energy per unit mass of water is proportional to the square of flow velocity. An indicator variable was assigned to each of the 16 reaches to represent particle

roughness. A value of 1 was assigned where a reach contained clastic sediment, and a value of zero where it did not. Debris can be contributed by mass-wasting events, as in the case of the lower Ptarmigan stream, or by channel cutting through medial moraines, as in the case of the Vaughan Lewis-Gilkey streams. A second indicator variable was assigned to each reach to represent form roughness contributed by channel bed topography. A value of 1 was assigned where water surface undulations were in phase with channel bedform topography (upper flow regimes), and a value of zero where water surface undulations were out of phase (lower flow regime) (Harms and Fahnstock 1965; Simons 1969). Sinuosity and variance of hydraulic radius data serve as an index of form roughness attributed to channel pattern and cross-sectional shape, respectively. Froude numbers range from 0.57 to 2.14, with values for four of the 16 reaches exceeding unity.

Values of Manning's roughness coefficient n were calculated for each reach in the Ptarmigan supraglacial stream using field data for velocity, hydraulic radius, and channel slope. The minimum value obtained for n was 0.013 for a debris-free reach with water surface undulations in phase with ice bedforms, a sinuosity of 1.05, a width of 21 cm, and a depth of 0.4 cm. An n value of 0.013 is below values found in natural streams but approaches n values for artificial concrete-lined channels (Chow 1959). The maximum value obtained for n was 0.039 for a reach with debris where the water surface undulations are out of phase with ice bedforms, a sinuosity of 1.25, a width of 14 cm, and a depth of 1 cm. An n value of 0.039 is typical of clean, meandering, minor alluvial streams with pools and riffles, or a major jagged and irregular channel carved in bedrock (Chow 1959). The mean n value of 0.022 is slightly lower than expected for natural, straight streams with minimal bed topography. The considerable range in n values and shifting importance of various roughness elements belie reported characterizations of supraglacial streams as homogeneous, free of clastics, and in the upper flow regime (Parker 1975; Park 1981).

A correlation matrix of roughness elements is presented for the lower Ptarmigan stream using indices described earlier (Table 2). The high degree of interdependence is not sur-

Table 2. Relationship Between Elements of Channel Roughness

	CBM	CBF	SIN	HYR	MAN
Channel Bed Material (CBM)	1.000	-0.856 0.001*	0.446 0.042	0.604 0.007	0.576 0.010
Channel Bedforms (CBF)		1.000	-0.631 0.004	-0.732 0.001	-0.714 0.001
Sinuosity (SIN)			1.000	0.913 0.001	0.901 0.001
Hydraulic Radius (HYR)				1.000	0.958 0.001
Manning's n (MAN)					1.000

* Probability that $r = 0.0$ in the population.

prising for stream systems but does preclude multiple regression. Along-the-reach variation in hydraulic radius provides the best single estimator of Manning's n (SE = 0.002), followed by sinuosity (SE = 0.003). Numerous equations are presented in the literature for estimating Manning's n with selected key variables, usually involving hydraulic radius and particle size (Gardiner and Dackombe 1983). The component method proposed by Cowen (1956) for estimating n assigns an index number to each roughness element outlined by Marston (1982), but values appropriate for supraglacial streams are not given. Further studies of roughness characteristics in supraglacial streams that replace qualitative indices with quantitative data will better define the relative contribution of individual roughness elements to the overall flow resistance.

Cross-Section Morphology

At-a-station hydraulic geometry data are presented for the three Vaughan Lewis-Gilkey supraglacial streams using methods described by Leopold and Maddock (1953) (Fig. 6). Mean values for the hydraulic geometry exponents are as follows: $\bar{b} = 0.097$, $\bar{f} = 0.433$, and $\bar{m} = 0.47$. As discharge increases in streams with the aforementioned exponents, the width-to-depth ratio decreases, competence increases, the Froude number increases, and the slope-to-roughness ratio increases (Rhodes 1977). The fact that f is greater than b indicates the channel bed is

more easily eroded than the banks. Indeed, daily lateral cutting ranges from 17 to 75 percent of daily downcutting by thermal erosion in the three Vaughan Lewis-Gilkey streams. The low b value is also typical of a straight channel reach, the pattern found at stations on all three Vaughan Lewis-Gilkey streams.

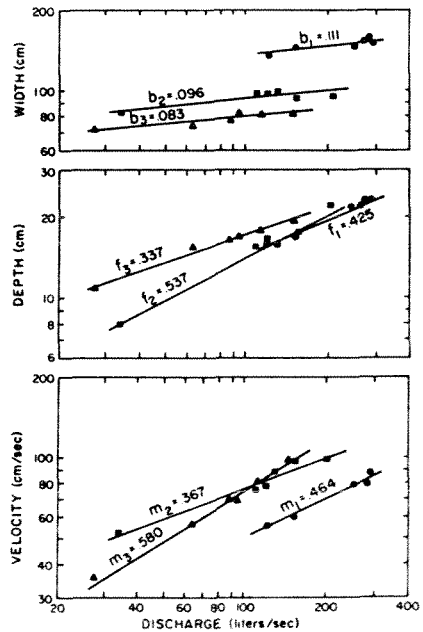


Figure 6. Hydraulic geometry for the three supraglacial streams in the Vaughan Lewis-Gilkey Glacier Research Area.

The meander wavelength-channel width relationships described earlier for the lower Ptarmigan stream also confirm this relationship (Fig. 5).

Small fluctuations in stream width with diurnal cycles in discharge account for a series of longitudinal grooves on supraglacial channel walls parallel to the channel slope (Fig. 7). As meltwater production and discharge increase, lateral thermal erosion expands active channel width concurrent with downcutting. As supraglacial runoff is suppressed, stream width decreases but downcutting continues. The resulting cusped-shaped channel banks are truncated the following morning as discharge rises again. Horizontal groove depth correlates most closely with total daily discharge ($r = 0.946$; Table 1). Vertical groove depth correlates most closely with peak daily discharge ($r = 0.871$). Longitudinal grooves may be considered intrinsic to supraglacial streams only in

the sense that such streams experience diurnal flow patterns and rapid downcutting, and have banks of ice capable of supporting concave slopes steeper than the angle of internal friction for earth materials. The supraglacial cross-section profile with cusped banks and flat bed is proposed as an equilibrium shape (Pinchak 1972a, 1972b). The channel enlargement ratios discussed earlier may be theoretically explained by the relative distribution of frictional heat on the channel perimeter. However, the values of b , f , and m for supraglacial streams in the present study are not unlike values reported for a number of alluvial streams with low sinuosity and small hydraulic radius (Rhodes 1977). Streams in contrasting climatic-hydrologic regimes may have similar b , f , and m values (Richards 1982). Therefore, fluvial adjustments toward an equilibrium condition must consider all elements of channel roughness, not just channel cross-section shape.

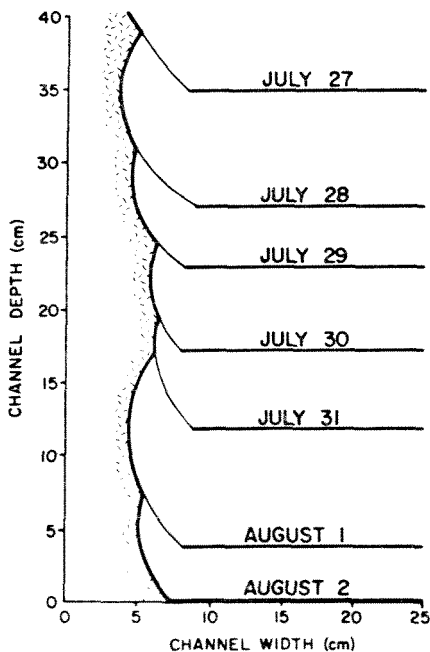


Figure 7. Horizontal grooves on channel walls corresponding to former active cross-sections in one of the supraglacial streams in the Vaughan Lewis-Gilkey Glacier Research Area.

Summary and Conclusions

The present study identifies sources, pathways, and temporal aspects of supraglacial runoff as a precursor to understanding supraglacial stream morphology. Supraglacial meltwater production exhibits a strong diurnal pattern, with peak and total daily discharge dependent on downward sky radiation. Supraglacial channels are established below the névé line where downcutting exceeds glacier surface ablation. Channel incision occurs by thermal erosion at rates of 4 to 8 cm/day from heat supplied by shortwave radiation, sensible heat flux from the air to the stream, and frictional heat from flow energy dissipation. The latter source of heat accounts for 50 to 75 percent of incision rates. Supraglacial streams leave the glacier surface via moulins and crevasses, contributing water to englacial and subglacial portions of the glacio-hydrologic drainage system.

Meandering supraglacial stream segments develop with small wavelengths and amplitudes but display form-process adjustments similar to those described for alluvial meander belts. However, ice structures can create a density barrier to downstream migration of supraglacial meanders, just as resistant clays cause alluvial meanders to pile

up in the downvalley direction. Time and scale are clearly not important in meander development. Sediment load is not necessary to initiate meanders in supraglacial streams, but the presence of clastics in the active channel can alter meander dimensions. Asymmetrical helical flow is cited as the mechanism for differential melting and freezing in supraglacial meanders. Water surface superelevation against one bank could provide the incremental frictional heat for thermal erosion. Sinuosity varies inversely with stream power within a given reach, but sinuosity increases in the downstream direction when the adjacent upstream reach supplies a higher stream power.

Systematic analyses of channel roughness characteristics are undertaken for supraglacial streams that have a diverse assemblage of roughness elements. Adjustment of channel pattern and cross-section shape to imposed stream power is affected by the simultaneous adjustments in other roughness elements. Hydraulic geometry data demonstrate that supraglacial streams respond to fluctuating discharge in a manner not unlike alluvial streams with cohesive bank materials. The cusate form of supraglacial channel banks deserves more attention as an adjustment toward equilibrium conditions in concert with adjustments in other roughness elements. Future studies by the author will attempt to measure temperature differences in the water column or otherwise demonstrate differential melting and refreezing in supraglacial streams. Findings from the present study should encourage further research in alluvial streams that pursues comprehensive surveys of roughness elements and their interdependent adjustments toward equilibrium conditions.

Acknowledgments

The author wishes to acknowledge support from the National Science Foundation, Foundation for Glacier and Environmental Research, Juneau Icefield Research Program, and University of Idaho. Particular encouragement for the project was provided by Maynard M. Miller, Director of the Juneau Icefield Research Program since its inception in 1946, and Alfred C. Pinchak, Case Western Reserve University. Expert field assistance under difficult conditions was provided by Erik Peterson, Brian Palmer, Eric DeFreest, and Andrew Nousen. The cartography is by Linda M. Marston.

Note

1. Lemon Creek Glacier served as one of the glaciological stations in the North American network during the International Geophysical Year, 1957–1958. Important contributions to the Juneau Icefield Research Program have been made by physical geographers during the International Geophysical Year and in years since, the most notable being work by Melvin G. Marcus, now of Arizona State University (Huesser and Marcus 1960, 1964a, 1964b; Marcus 1960, 1964). Research was conducted by the American Geographical Society with support from the Office of Naval Research between 1948 and 1958. Findings are summarized in a series of general reports (American Geographical Society 1953–58). Subsequent funding has been obtained at various times from the National Geographic Society, Michigan State University, and agencies listed in the acknowledgments.

References

- American Geographical Society.** 1953–58. *Juneau Icefield Research Project. Progress and Semi-Annual Status Reports.* New York: American Geographical Society.
- Asher, R. A., Miller, M. M., McCracken, J., and Petrie, C.** 1974. *An unusual glacier cave in the Lemon Glacier, Alaska—an englacial drainage and reservoir system.* Center for Short-Lived Phenomena, Smithsonian Institution, Washington, D.C.
- Chow, V. T.** 1959. *Open-channel hydraulics.* New York: McGraw-Hill.
- Clayton, L.** 1964. Karst topography on stagnant glaciers. *Journal of Glaciology* 5:107–12.
- Cowen, W. L.** 1956. Estimating hydraulic roughness coefficients. *Agricultural Engineering* 37:473–75.
- Dewart, G.** 1966. Moulins on Kaskawalsh Glacier, Yukon Territory. *Journal of Glaciology* 6:320–21.
- Dozier, J.** 1976. An examination of the variance minimization tendencies of a supraglacial stream. *Journal of Hydrology* 31:359–80.
- Ferguson, R. I.** 1973. Sinuosity of supraglacial streams. *Geological Society of America Bulletin* 84:251–56.
- Gardiner, V., and Dackombe, R.** 1983. *Geomorphological field manual.* London: George Allen & Unwin.
- Glen, J. W.** 1954. The stability of ice-dammed lakes and other water-filled holes in glaciers. *Journal of Glaciology* 2:316–18.
- Harms, J. C., and Fahnstock, R. K.** 1965. Stratification, bed forms and flow phenomena, with an example from the Rio Grande. In *Primary sedimentary structures*, ed. G. V. Middleton, pp. 84–115. Tulsa: Society of Economic Paleontologists and Mineralogists.
- Huesser, C. J., and Marcus, M. G.** 1960. *Glaciological and related studies of Lemon Creek Glacier, Alaska.* Juneau Icefield Research Project,

- Final Report. New York: American Geographical Society.
- . 1964a. Historical variations of Lemon Creek Glacier, Alaska, and their relationship to the climatic record. *Journal of Glaciology* 5:77–86.
- . 1964b. Surface movement, hydrological change and equilibrium flow on Lemon Creek Glacier, Alaska. *Journal of Glaciology* 5:61–75.
- Howarth, P. J.** 1968. A supraglacial extension of an ice-dammed lake, Tunsbergdalsbreen, Norway. *Journal of Glaciology* 7:413–19.
- Knighton, A. D.** 1972. Meandering habit of supraglacial streams. *Geological Society of America Bulletin* 83:201–4.
- Kolb, C. R.** 1963. Sediments forming the bed and banks of the lower Mississippi River and their effects on river migration. *Sedimentology* 2:227–34.
- Leopold, L. B., and Maddock, T.** 1953. The hydraulic geometry of stream channels and some physiographic implications. U.S. Geological Survey Professional Paper 252, Washington, D.C.
- Leopold, L. B., and Wolman, M. G.** 1960. River meanders. *Geological Society of America Bulletin* 71:769–94.
- Marcus, M. G.** 1960. Periodic drainage of glacier-dammed Tulsequah Lake, British Columbia. *Geographical Review* 50:89–106.
- . 1964. *Climate-glacier studies in the Juneau Icefield region, Alaska*. Department of Geography Research Paper 88. Chicago: University of Chicago.
- Marston, R. A.** 1982. The geomorphic significance of log steps in forest streams. *Annals of the Association of American Geographers* 72:99–108.
- Miller, M. M.** 1963. *Taku Glacier evaluation study*. Alaska Department of Highways, Juneau, Alaska.
- . 1964. Inventory of terminal position changes in Alaskan coastal glaciers since the 1750's. *Proceedings of the American Philosophical Society* 108:257–73.
- . 1975. *Mountain and glacier terrain study and related investigations in the Juneau Icefield region, Alaska-Canada*. Foundation for Glacier and Environmental Research, Monograph Series. Seattle, Wash.
- Park, C. C.** 1981. Hydraulic geometry of a supraglacial stream—some observations from the Val d'Herens, Switzerland. *Revue de Géomorphologie Dynamique* 30:1–9.
- Parker, G.** 1975. Meandering of supraglacial melt streams. *Water Resources Research* 11:551–52.
- . 1976. On the cause and characteristic scale of meandering and braiding in rivers. *Journal of Fluid Mechanics* 76:459–80.
- Pinchak, A. C.** 1972a. *Diurnal flow variations and thermal erosion in supraglacial streams*. Institute of Water Research, Michigan State University, Technical Report 33, Part XII, East Lansing, Mich.
- . 1972b. Some observations of supraglacial meltwater streams on the Gilkey and Vaughan Lewis Glaciers, Alaska. Paper read at Arctic and Mountain Environments Symposium, 22-23 April, at Michigan State University, Lansing, Michigan.
- Price, R. J.** 1973. *Glacial and fluvio-glacial landforms*. New York: Hafner.
- Rhodes, D. D.** 1977. The *b-f-m* diagram—graphical representation and interpretation of at-a-station hydraulic geometry. *American Journal of Science* 277:73–96.
- Richards, K.** 1982. *Rivers-form and process in alluvial channels*. London: Methuen.
- Rothlisberger, H.** 1972. Water pressure in intra- and subglacial channels. *Journal of Glaciology* 11:177–203.
- Schumm, S. A.** 1977. *The fluvial system*. New York: Wiley-Interscience.
- Shahjahan, M.** 1970. Factors controlling the geometry of fluvial meanders. *International Association of Scientific Hydrology Bulletin* 15:13–24.
- Simons, D. B.** 1969. Open channel flow. In *Introduction to physical hydrology*, ed. R. J. Chorley, pp. 131–52. London: Methuen.
- Streff-Becker, R.** 1951. Pot-holes and glacier mills. *Journal of Glaciology* 1:488–90.
- Zeller, J.** 1967. Meandering channels in Switzerland. *International Association of Scientific Hydrology Publication* 75:174–86.